A CMOS Photodiode Model

Wei-Jean Liu, Oscal T.-C. Chen
Signal and Media Laboratories,
Dept. of Electrical Engineering,
National Chung Cheng University,
Chia-Yi, 621Taiwan

Li-Kuo Dai, Ping-Kuo Weng, Kaung-Hsin Huang, Far-Wen Jih
Solid-State Devices Materials Section,
Materials & Electro-Optics Research Division,
Chung-Shan Institute of Science & Technology,
Tao-Yuan, Taiwan

■ **Abstract**

This paper utilizes the concepts of equilibrium equations and minority carrier continuity to build and derive at a CMOS photodiode model. By using the TSMC 1P3M 0.5 μ m CMOS technology, photodiodes with two different types of N_{well}-$P_{Epitaxial}$-$P_{substrate}$ and $N_{diffusion}$-P_{well}-$P_{Epitaxial}$-$P_{substrate}$ were fabricated. Measurements were done to test the photoresponse from 400nm to 1000nm. To simulate the photoresponses of the N_{well}-$P_{Epitaxial}$-$P_{substrate}$ and $N_{diffusion}$-P_{well}-$P_{Epitaxial}$-$P_{substrate}$ photodiodes using the proposed model, if an inadequate value of the surface recombination velocity which is affected by the surface defects in the manufacture process is utilized, the proposed model would yield a little larger error in estimating the photoresponse in a shorter wavelength. To overcome this problem, the curve mapping scheme is applied to find the adequate boundary condition of the surface recombination velocity with the least mean squared error thus allowing the proposed model to achieve a good performance. The concept of the model proposed herein could be utilized in designing any CMOS photodiode for simulating its photo-electronic characteristics in various industrial applications.

1. Introduction

The CMOS process has increasingly becoming the mainstay in the IC market due to advantages of its low-power dissipation and high-density integration. Its applications will also be more prevalent as the photo-electronic conversion becomes one of the enabling technologies. Figure 1(a) illustrates a conventional photodiode with a single layer [1]. However with advances in technologies, multi-layers as shown in Fig. 1(b) and 1(c) are now available and prevailing. This work conducts a complete analysis, simulation and measurement of the photo response characteristics of the CMOS photodiode. First, the physic characteristics of the semiconductor will be analyzed. With equilibrium equations and adequate boundary conditions, a CMOS photodiode model useful in any architecture design will be derived. Next the 1P3M CMOS 0.5 μ m process provided by the TSMC is used to design photodiodes with two different types of N_{well}-$P_{Epitaxial}$-$P_{substrate}$ and $N_{diffusion}$-P_{well}-$P_{Epitaxial}$-$P_{substrate}$. Measurements are then done to test their photo responses. Lastly, the results from measurement and simulation are compared and analyzed. By using the curve mapping scheme to find the adequate boundary condition with the least mean squared error, the proposed model would be able to achieve an optimized performance. Therefore, the CMOS photodiode model proposed herein can be integrated with various circuit simulators to provide system-on-chip simulations of industrial apapplications with CMOS sensors.

2. The Proposed CMOS Photodiode Model

Photo current happens because incident light incites electron-hole pairs. When a potential applied on two sides of a photodiode separates the electron-hole pairs, the photo current is generated. Two major sources of photo currents are: (1) from the diffusion current due to an imbalance of carrier concentration outside of the depletion region; (2) from the drift current due to the separation of electron-hole pairs within the electric field of the depletion region. In analyzing the physic characteristics of a semiconductor, there are two assumptions in general: (1) electric field outside of the depletion region is set to zero, meaning that drift current only happens within the depletion region; (2) the state of low-level injection, meaning that the variation of majority carrier concentration can be neglected.

A few parameters must be illustrated before going into details on deriving a CMOS photodiode model. First the "excess minority generation rate" using the function of $G(x, \lambda)$ represents the number of excess minority carrier produced within each unit, 1/(cm$^3\times$ sec). The x represents the depth of the distance from the incident light contact area of the semiconductor, while λ stands for the wavelength of the incident light. This mathematical function explains that the excess minority generation rate is a function of the incident wavelength and the depth of distance from the incident light contact area. When x is at the depth of the distance from the contact area of the semiconductor, exponential decay would happen to excess minority generation rate $G(x, \lambda)$ as shown below:

$$G(x,\lambda) = \varphi(x)\times\alpha\times\exp(-\alpha x) \tag{1}$$

The parameter of $\varphi(x)$ is a photon flux, and x indicates the distance away from the incident surface. An exponential decay following this distance will happen. If $\varphi(0)$ means the photon flux at the incident surface, $\varphi(0)$ and $\varphi(x)$ have the following relationship:

$$\varphi(0) = \frac{P_{in}}{h\nu}(1-R) \tag{2}$$

$$\varphi(x) = \varphi(0)\times\exp(-\alpha x) \tag{3}$$

Where R is a reflection rate, h is the Planck constant, P_{in} is the power of incident light, ν is the frequency of incident light, and α is the absorption coefficient of the photo-receiving material. The absorption coefficient is an inverse of the absorption length that indicates the length where the photon flux decays to 1/e of the previous one. For the silicon material, the relationship between the absorption length and light wavelengths is shown in Figure 2. If the wavelength is λ, then α could be represented by [2]:

$$\log_{10}\alpha = 13.2131 - 36.7985\lambda + 48.1893\lambda^2 - 22.7562\lambda^3 \quad (4)$$

In deriving the proposed CMOS photodiode, the basic structure as shown in Figure 1(a) is adopted first. As this research assumed from the beginning that the electric field could only exist within the depletion region, the drift current then could only be generated within the depletion region. This is possible by performing integration on the length of the depletion region based on the carrier generation rate to get the number of all carriers. Each carrier is then multiplied by its electron charge to derive at the intensity of the drift current within the depletion region, as shown below:

$$J_{drift} = -q\int_{x_n}^{x_d} G(x,\lambda)dx \quad (5)$$

Next the diffusion current, caused by the density imbalance outside of the depletion region, is derived. As the photocurrent is generated from the minority carrier, we can study its behavior at the equilibrium state. In an N-type semiconductor where hole is the minority carrier, the equilibrium equation is:

$$D_p \frac{d^2(p_n(x)-p_{n0})}{dx^2} - \frac{p_n(x)-p_{n0}}{\tau_p} + G(\lambda,x) = 0 \quad (6)$$

In Eq. (6), P_{n0} represents the density of the minority carrier (hole) when the N-type semiconductor is at the equilibrium state; P_n is all the minority carrier concentration after light incident; D_p as the hole's diffusion coefficient and τ_p as lifetime of the hole. After deriving the general solution, two sets of boundary condition must be included to derive the particular solution. The first set of boundary condition is at the surface area of x being 0:

$$D_p \times \frac{\partial(p_n(x)-p_{n0})}{\partial x} = \left[-\left(p_n(x)-p_{n0}\right)\times S_p\right]_{x=0} \quad (7)$$

The S_p in Equation (7) is the surface recombination velocity of the hole at the semiconductor's surface area. For the purpose of simulation simplicity, this parameter is firstly set to infinity to derive at the boundary condition of $P_n(0)$ being equal to P_{n0}. The second set of boundary condition would be the boundary condition on the edges of the depletion region of x being x_n. Assuming the low-level injection, the boundary condition is represented by the following:

$$p_n(x_n) = p_{n0}e^{\left(-\frac{qV_{bias}}{kT}\right)} \quad (8)$$

V_{bias} is the inverse-biased voltage added at the two sides of the photodiode, k as the Boltzmann constant, and T as the absolute temperature. The particular solution of $P_n(X)$ could then be derived using these two sets of boundary conditions. Lastly, incorporating the expression below would achieve the current density generated in an N-type semiconductor:

$$J_n = qD_p\left(\partial p_n/\partial x\right)_{x=x_n} \quad (9)$$

Similarly, the current density in a p-type semiconductor could also be derived using the equilibrium equation as in Eq. (10) along with Eq. (11) representing the bottom layer of the semiconductor and Eq. (12) as the boundary condition beneath the depletion region.

$$D_n \frac{d^2(n_p(x)-n_{p0})}{dx^2} - \frac{n_p(x)-n_{p0}}{\tau_n} + G(\lambda,x) = 0 \quad (10)$$

$$D_n \times \frac{\partial(n_p(x)-n_{p0})}{\partial x} = \left[-\left(n_p(x)-n_{p0}\right)\times S_n\right]_{x=x_h} \quad (11)$$

$$n_p(x_d) = n_{p0}e^{\left(-\frac{qV_{bias}}{kT}\right)} \quad (12)$$

As in Eq. (13), photo currents generated by the p-type semiconductor could be accomplished. Note that the carriers considered here are electrons, with signs opposite of J_n.

$$J_p = -qD_n\left(\partial n_p/\partial x\right)_{x=x_d} \quad (13)$$

The above equations only solve the simplest photodiode model shown in Figure 1(a). Next, in comparing the CMOS photodiodes shown in Figure 1(b) and Figure 1(c) with a conventional one, the most significant difference is the multi-layer structure in the p-type semiconductor. Where the two P layers meet in the N_{well}-$P_{Epitaxial}$-$P_{substrate}$ photodiode as shown in Figure 1(b), the new boundary condition is generated. This boundary condition could be looked at from the physic characteristics of the current density and minority carrier concentration. First look at the current density. Due to the continuity of currents, the current densities at where the two layers meet would be equal thus creating the first boundary condition as follows:

$$J = -q\times D_{n1}\times\left(\frac{\partial n_{p1}}{\partial x}\right)_{x=x_p} = -q\times D_{n2}\times\left(\frac{\partial n_{p2}}{\partial x}\right)_{x=x_p} \quad (14)$$

D_{n1} and D_{n2} represent the diffusion coefficients in $P_{Epitaxial}$ and $P_{substrate}$, respectively, whereas n_{p1} and n_{p2} are the densities of the minority carriers in $P_{Epitaxial}$ and $P_{substrate}$, respectively. The second boundary condition is achieved from the continuity of concentration of the minority carrier, as shown below:

$$n_{p1}\left[x_p\right] = n_{p2}\left[x_p\right] \quad (15)$$

It is evident to see that from using the continuity relationship of the current density and minority carrier concentration, the photo current equation of a multi-layer photodiode could be solved. Hence, to derive the model of the $N_{diffusion}$-P_{well}-$P_{Epitaxial}$-$P_{substrate}$ photodiode in Figure 1(c), the continuity of current density and minority carrier concentration between P_{well}-$P_{Epitaxial}$ and $P_{Epitaxial}$-$P_{substrate}$ can be utilized.

Lastly, one thing to note is the dark current. It is caused by many reasons, such as temperature, density, biased voltage, and defects in the manufacture process. The dark current concerned here is generated from bias voltage, and this term should be removed. To derive at the dark current generated by the biased voltage and carry densities, P_{in} of energy for incident light is set to 0 in the equation. The following equation derives the total current density, where J_{dark} stands for the dark current:

$$J_{total} = J_n + J_{drift} + J_p - J_{dark} \quad (16)$$

3. Simulation and Analysis of the Photodiode Models

The simulation of the photo responses of N_{well}-$P_{Epitaxial}$-$P_{substrate}$ and $N_{diffusion}$-P_{well}-$P_{Epitaxial}$-$P_{substrate}$ photodiodes is shown in Figure 3, and that at each region of the photodiodes is shown in Figure 4 and Figure 5. The effect of that the currents generated from these regions are quite different is made by the ionic doping concentration and doping depth. Doping concentration mainly affects the current density. The minority carriers, that need diffuse to the edge of the depletion region and then pass through this region, become photocurrents successfully. Hence, the more ionic doping concentration is the higher probability of minority recombination is. In other words, the induced current is decreased as the ionic doping concentration is increased[3]. We can observe that a greater ionic doping concentration causes a shorter minority carrier lifetime. In addition to doping concentration, the doping depth affects the absorption wavelength. From Figure 2, a longer wavelength can penetrate into a deeper region. Therefore, a deeper junction depth has a better photo response for a longer wavelength and vice versa. Here, we compare the photo responses of the above two photodiodes as shown in Figure 4 and Figure 5. Due to the N_{well} having a less doping concentration and a deeper depth than those of the $N_{diffusion}$,

the photo response of N_{well} has a greater value, and a response peak in a longer wavelength. Since the light wavelength nearby 400nm is absorbed more by the N_{well} region and less by the $N_{diffusion}$ region, the current density in the P-type semiconductor of the $N_{diffusion}$-P_{well}-$P_{epitaxial}$-$P_{substrate}$ photodiode has a better response in a short wavelength. When comparing photo responses of the N-type and P-type semiconductors, the P-type semiconductor has a less ionic doping concentration and a deeper depth, and thereby it has a large photo response to the incident light with a long wavelength.

4. Comparison of Measurement and Simulation Results

Figure. 6 illustrates the measurement results of the photo responses of these two photodiodes. The $N_{diffusion}$-P_{well}-$P_{epitaxial}$-$P_{substrate}$ photodiode shows a better response as we predicted in simulation. Next, simulation and measurement results are compared. Figure 7 shows the measured and simulated photo responses under a biased voltage being 0V and the surface recombination velocity being infinity. When a wavelength is less than 750nm, there is a larger difference between the simulation and measurement results. As previously mentioned, the surface recombination velocity affects the number of minority carriers generated by the minority carriers on surface contact areas. As explainable from Eqs. (7) and (11), if the surface recombination velocity is set at infinity, the two sets of boundary conditions then could take on the following expressions:

$$p_n(0)=p_{n0} \quad (17)$$

$$n_p(x_h)=n_{p0} \quad (18)$$

Equation (18) holds according to the law of physics. As shown in Figure 2, under the influence of the absorption coefficient, and the thickness of a few hundred micro meter for the entire CMOS photodiode, the minority carrier generated by the incident light is close to zero at the bottom of the semiconductor [4]. The minority carrier is actually the number of minority carrier under a balance state. However, it is impossible to make the number of minority carrier equal to zero at the top surface of the semiconductor. Hence, Eq. (17) may not be true. This means that there are always more minority carriers in this section than the number of minority carriers under a balance state. Setting the boundary condition at contact area of x being 0 is also another reason behind the difference between measurement and simulation. The effect of the surface recombination velocity is shown in Figure 8. The surface photocurrent yields the maximum when the surface recombination velocity is zero and zero when that is infinite. Figure 9 shows the photo responses from 400nm to 700nm under several different surface recombination velocities.

To improve upon this error, the curve mapping scheme is adopted to come up with a boundary condition set that allows the least mean squared error between simulation and measurement. After computation, the surface recombination velocity at contact areas for N_{well}-$P_{Epitaxial}$-$P_{substrate}$ and $N_{diffusion}$-P_{well}-$P_{epitaxial}$-$P_{substrate}$ photodiodes are 2×10^3(cm/sec) and 1×10^4(cm/sec), respectively. Table 1 lists the comparison of the proposed and conventional CMOS photodiode models[1]. The model proposed herein can accommodate many structures with adaptive parameters to achieve a precise estimation of photoresponse.

5. Conclusion

A CMOS photodiode model useful in all kinds of CMOS photodiode structures was accomplished. By using the TSMC 1P3M 0.5 μ m CMOS technology, photodiodes with two different types of N_{well}-$P_{Epitaxial}$-$P_{substrate}$ and $N_{diffusion}$-P_{well}-$P_{Epitaxial}$-$P_{substrate}$ were implemented. The simulation and measurements of these two photodiodes were conducted to find the optimized boundary conditions. It is evident that the proposed photodiode model would be useful in various circuit simulators to understand the responses of the CMOS photodiodes.

References

[1] J. Reginald and K. Arora, "Using PSPICE to simulate the photoresponse of ideal CMOS integrated circuit photodiodes," *Proc. of IEEE Southeastcon Bringing Together Education, Science and Technology*, pp. 374 –380, 1996.

[2] H. Melchior, "Demodulation and photodetection techniques," in *Laser Handbook Vol. 1,* F. T. Arecchi and E. O. Schulz-Dubios, Eds. Amsterdam:North Holland, pp. 725-835, 1972.

[3] D. Schroder., *Semiconductor Material and Device Characterization*, New York: John Wiley and Sons, 1990.

[4] S. Sze, *Physics of Semiconductor Devices*, New York: John Wiley and Sons, 1980.

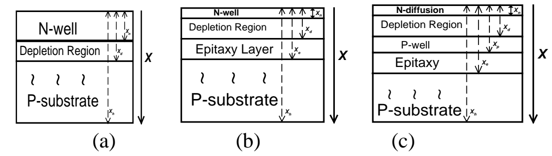

Fig.1 Cross sections of photodiodes.
(a)N_{well}-$P_{substrate}$.
(b)N_{well}-$P_{Epitaxial}$-$P_{substrate}$.
(c)$N_{diffusion}$-P_{well}-$P_{Epitaxial}$-$P_{substrate}$.

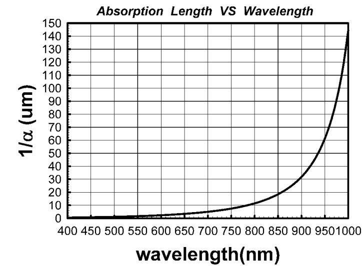

Fig.2 Relationship between absorption coefficients and wavelengths.

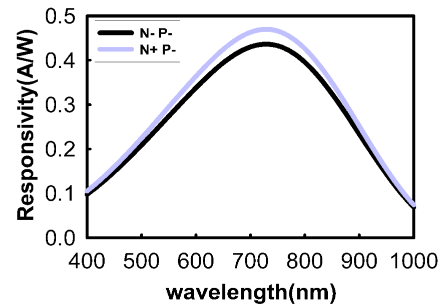

Fig.3 Simulation results of N_{well}-$P_{Epitaxial}$-$P_{substrate}$. and $N_{diffusion}$-P_{well}-$P_{Epitaxial}$-$P_{substrate}$ photodiodes.

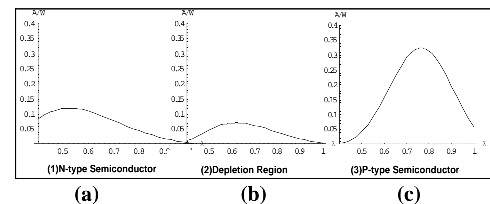

(a) **(b)** **(c)**

Fig.4 The simulated currents of the N_{well}-$P_{Epitaxial}$-$P_{substrate}$ photodiode in each region.

(a)N-type semiconductor.
(b)Depletion region.
(c)P-type semiconductor.

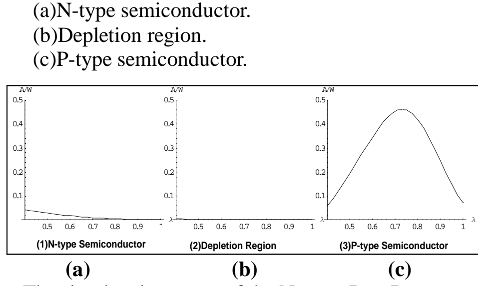

(a) (b) (c)

Fig.5 The simulated currents of the $N_{diffusion}$-P_{well}-$P_{Epitaxial}$-$P_{substrate}$ photodiode in each region.
(a)N-type semiconductor.
(b)Depletion region.
(c)P-type semiconductor.

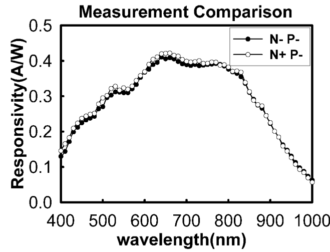

Fig.6 Measured responsivities of N_{well}-$P_{Epitaxial}$-$P_{substrate}$ and $N_{diffusion}$-P_{well}-$P_{Epitaxial}$-$P_{substrate}$ photodiodes.

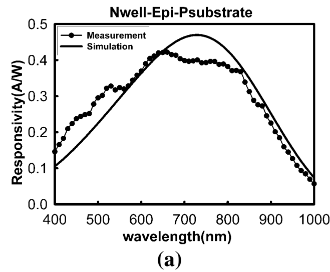

(a)

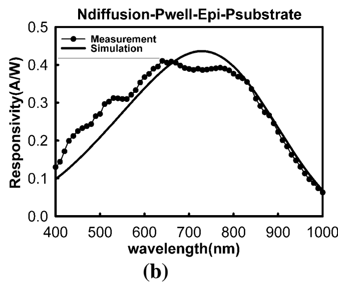

(b)

Fig.7 Measured and simulated responsivities for zero bias voltage and infinite surface recombination velocity .
(a) N_{well}-$P_{Epitaxial}$-$P_{substrate}$
(b) $N_{diffusion}$-P_{well}-$P_{Epitaxial}$-$P_{substrate}$

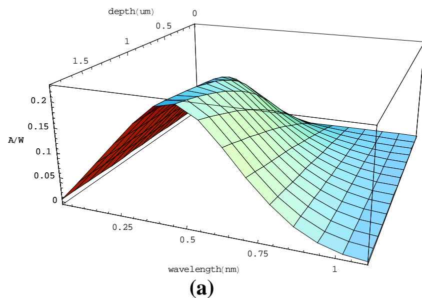

(a)

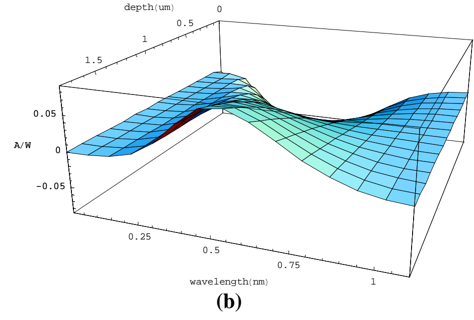

(b)

Fig.8 The effect of the surface recombination velocity to the current density in the semisonductor surface.
(a)Surface recombination velocity being ∞.
(b)Surface recombination velocity being 0.

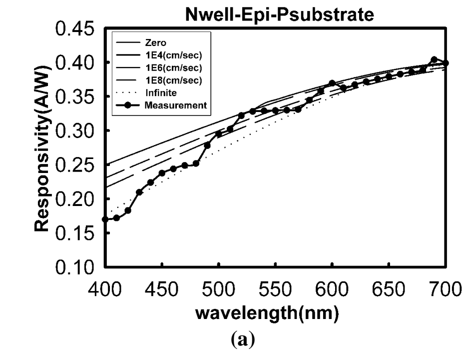

(a)

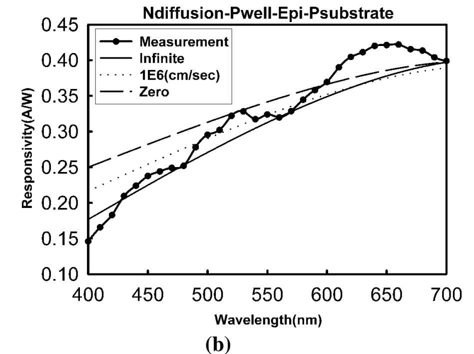

(b)

Fig.9 The photo responses from 400nm to 750nm under several different surface recombination velocities.
(a) N_{well}-$P_{Epitaxial}$-$P_{substrate}$
(b) $N_{diffusion}$-P_{well}-$P_{Epitaxial}$-$P_{substrate}$

Table 1. The comparison of the proposed and the conventional models.

Conditions \ Models		Conventional CMOS photodiode model[1]	The proposed model
Parameter consideration	Surface recombination velocity	Infinite	Utilizing curve mapping to find the adequate value
	Bias voltage	Zero only	Any value
	Dark current from bias voltage	Neglect	Dependent on bias voltage
Structures		Single layer only	Adaptive for all kinds of photodiodes